SUPPLEMENTAL DATA

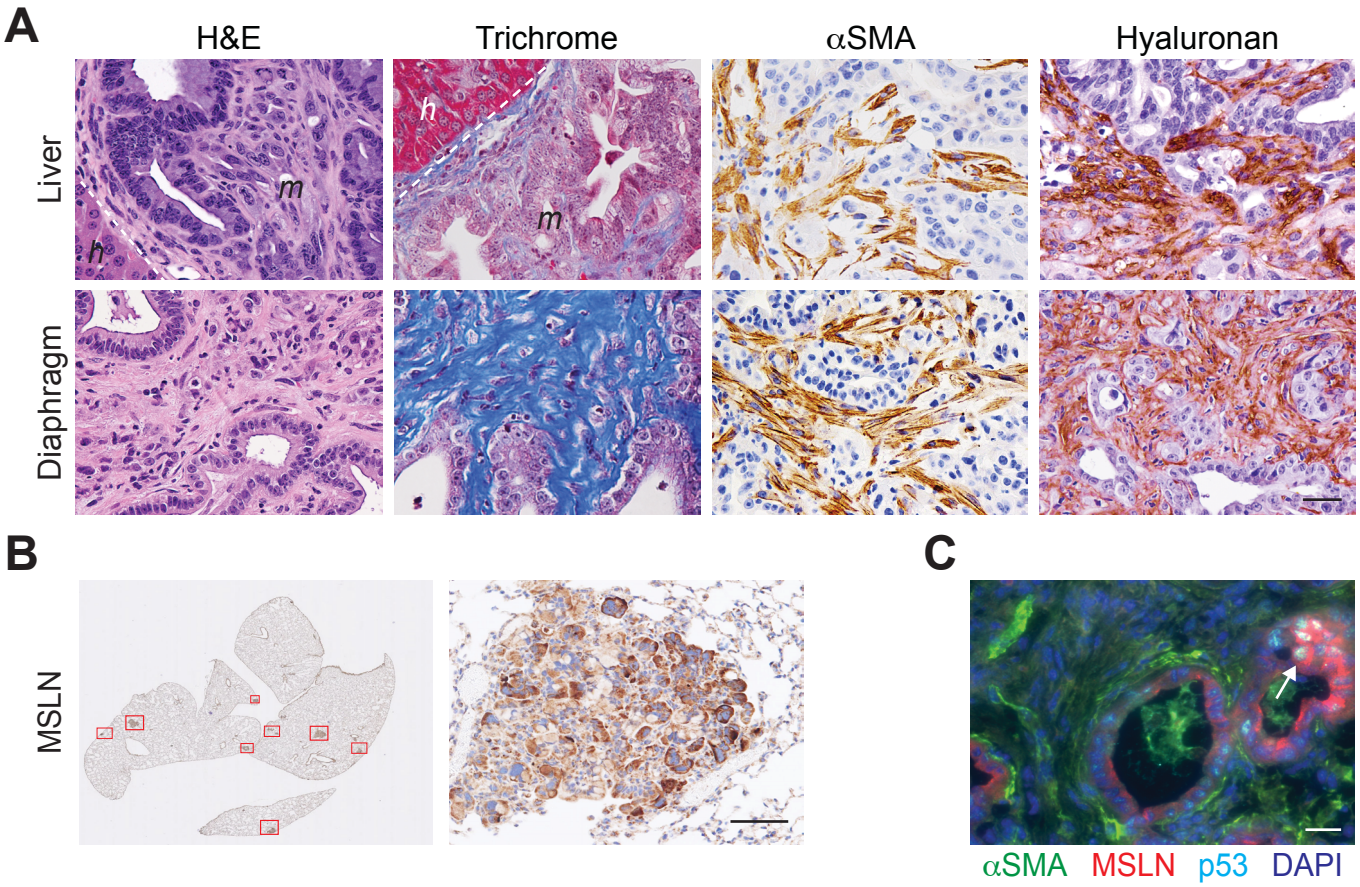

Figure S1, related to Figure 1.
(A) Histology of liver and diaphragm metastases in B6 *KPC* mice. h, hepatocytes; m, metastasis. Scale bar, 25 μm.
(B) MSLN expression in lung micrometastases. Scale bar, 25 μm.
(C) $p53^+$ cells and not αSMA^+ cells express MSLN. Arrow, $MSLN^+p53^+$ cells. Scale bar, 25 μm.
(D) MSLN expression in normal tissues and PDA. Arrows, rare $MSLN^+$ cells in thymus, pleura and pericardium; *, tumor epithelial cells. Scale bar, 50 μm.
(E) MSLN mRNA in the indicated tissues.
(F) MSLN mRNA in tumor cells normalized to levels in thymus.
Data are shown as mean ± SEM.

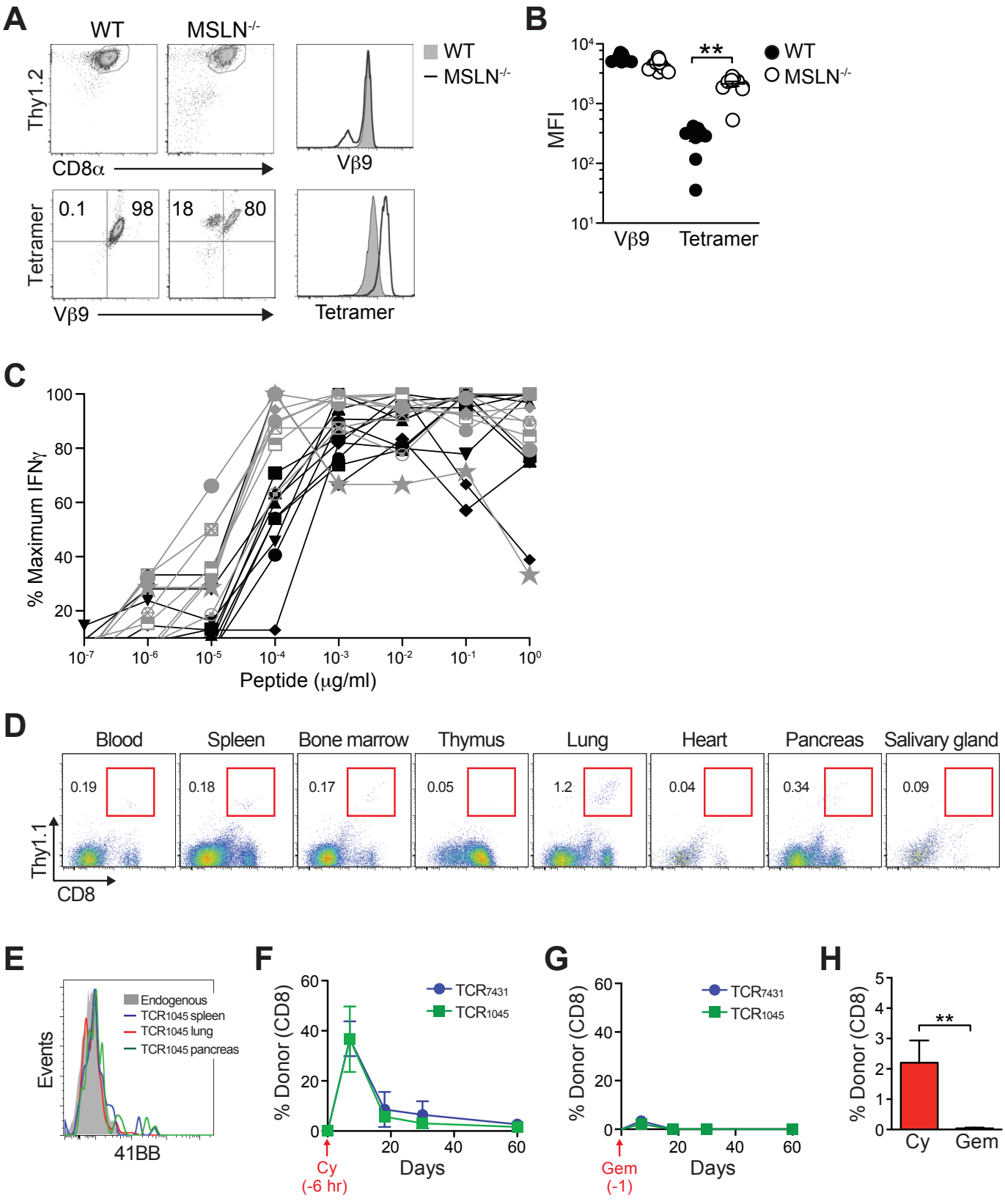
A
WT
MSLN-/-
Thy1.2
CD8α
Vβ9
Tetramer
0.1
98
18
80
WT
MSLN-/-
B
MFI
**
WT
MSLN-/-
Vβ9
Tetramer
C
% Maximum IFNγ
Peptide (μg/ml)
D
Blood
Spleen
Bone marrow
Thymus
Lung
Heart
Pancreas
Salivary gland
0.19
0.18
0.17
0.05
1.2
0.04
0.34
0.09
Thy1.1
CD8
E
Events
Endogenous
TCR1045 spleen
TCR1045 lung
TCR1045 pancreas
41BB
F
% Donor (CD8)
TCR7431
TCR1045
Cy
(-6 hr)
Days
G
% Donor (CD8)
TCR7431
TCR1045
Gem
(-1)
Days
H
% Donor (CD8)
**
Cy
Gem

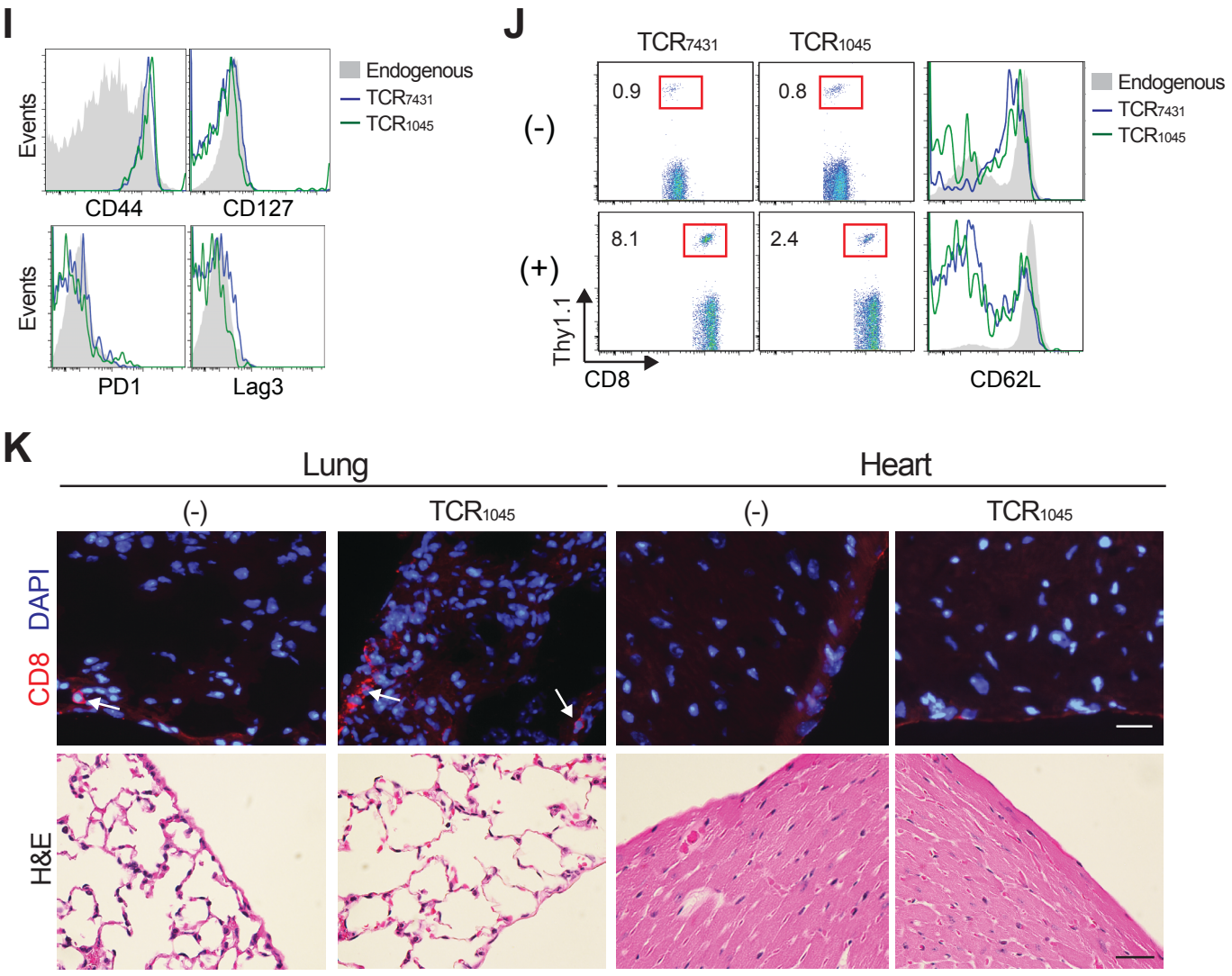

Figure S2, related to Figure 2.
(A) TCR (Vβ9) and $MSLN_{406-414}$/H-$2D^b$ tetramer staining of T cell lines from $MSLN^{-/-}$ and WT mice.
(B) Mean fluorescence intensity (MFI) of TCR (Vβ9) and tetramer of T cell clones.
(C) Dose response of T cell clones derived from $MSLN^{-/-}$ (grey) or WT (black) mice. Data are normalized to maximum $CD8^+$ T cell IFNγ production.
(D) Frequency of donor TCR_{1045} cells in WT mice 8 days following administration of twice-stimulated TCR_{1045} cells ($1x10^7$) and IL-2. Plots are gated on $CD45^+$ cells.
(E) 41BB expression by TCR_{1045} cells 8 days post infusion.
(F) Frequency of circulating donor T cells following cyclophosphamide (Cy, 180 mg/kg) 6 hr prior to cell infusion (-6 hr). Mice also received IL-2 and irradiated peptide-pulsed splenocytes ($1x10^7$).
(G) Circulating donor T cell frequency following gemcitabine (Gem, 100 mg/kg) 1 day prior to cell infusion (-1). Mice received IL-2 and antigen as described (Figure S2F).
(H) Frequency of circulating donor TCR_{1045} cells 60 days post infusion from conditioned mice.
(I) Circulating donor TCR_{1045} cells have a resting phenotype 60 days post infusion.
(J) Splenic memory donor T cells expand and downregulate CD62L 7 days post immunization (d.p.i.) with Ad-MSLN (+) but not control vaccine (-).
(K) CD8 T cell localization and lack of pathology in lung and heart 7 d.p.i from mice in Figure S2J. Arrows, $CD8^+$ T cells in lung. Scale bar, 25 μm (top), 50 μm (bottom).
Data are shown as mean ± SEM and representative of n=3-5 mice each.

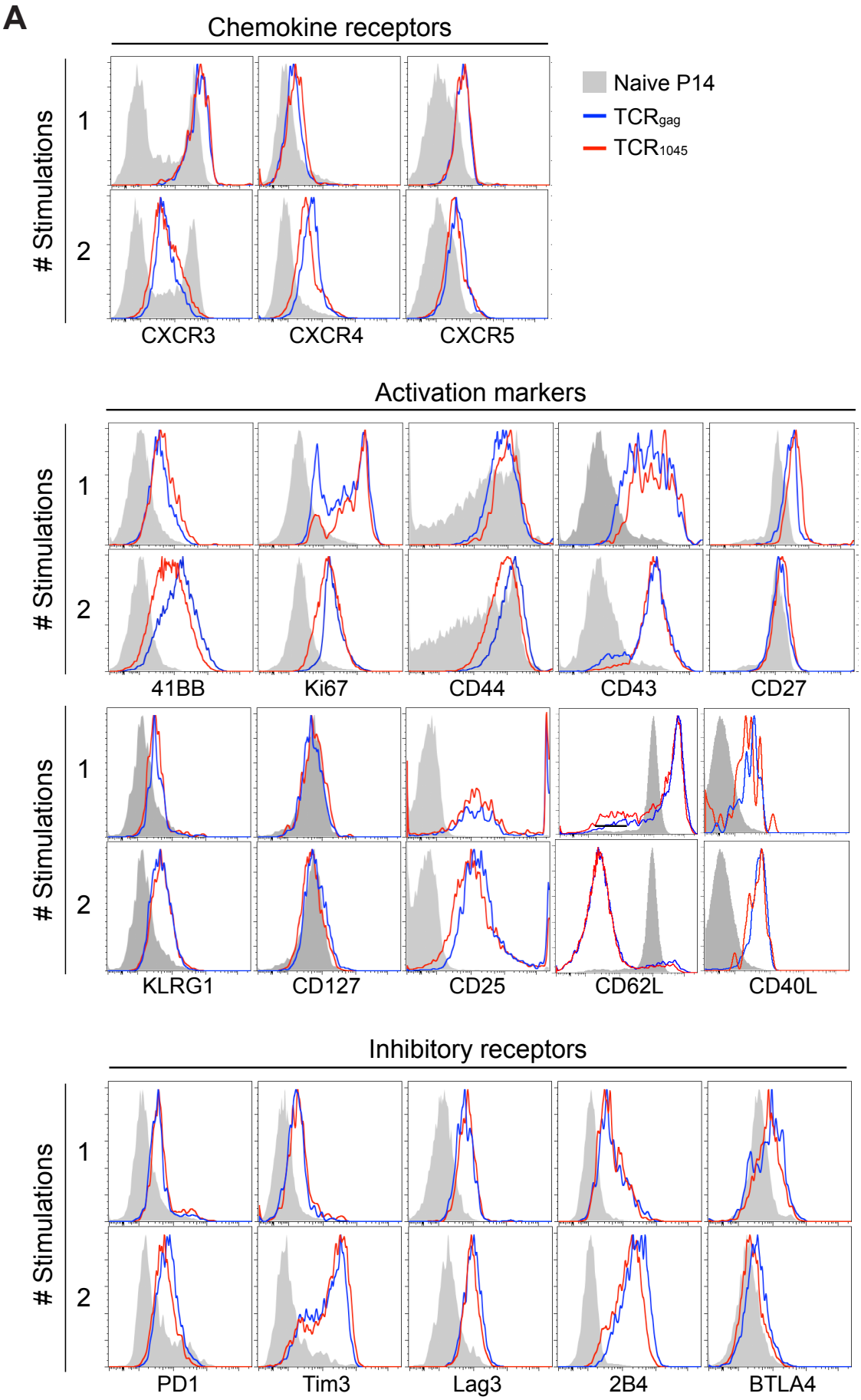
A
Chemokine receptors
Stimulations
1
2
CXCR3
CXCR4
CXCR5
Naive P14
TCRgag
TCR1045
Activation markers
41BB
Ki67
CD44
CD43
CD27
KLRG1
CD127
CD25
CD62L
CD40L
Inhibitory receptors
PD1
Tim3
Lag3
2B4
BTLA4

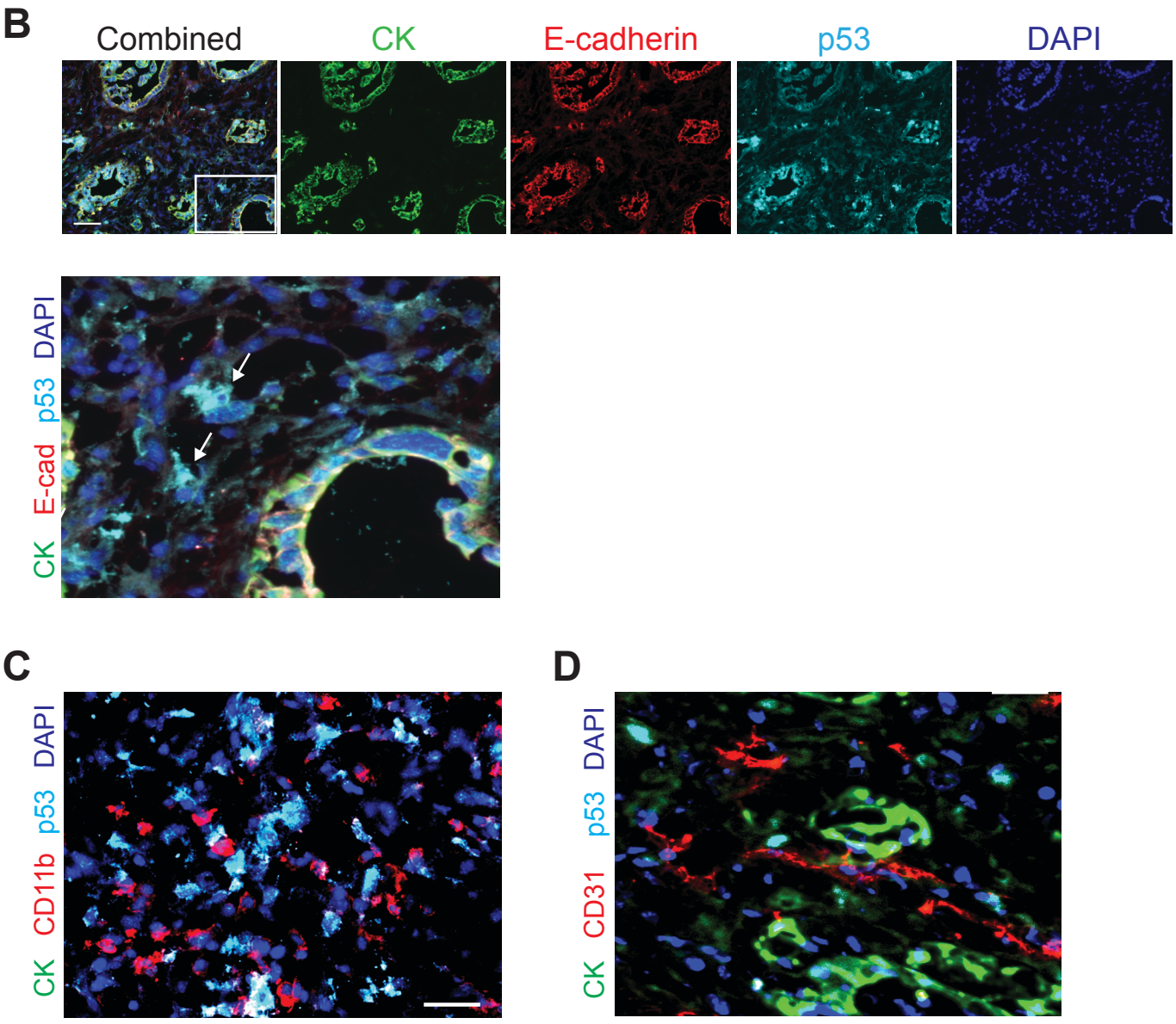

Figure S3, related to Figure 3.
(A) Phenotype of transduced TCR_{1045} and TCR_{gag} T cells 5 days following 1 or 2 in vitro stimulations with antigen and IL-2.
(B) $p53^+$ cells in stroma do not express E-cadherin or CK. Inset (white box) is shown magnified below. Arrows, $E\text{-cadherin}^-CK^-p53^+$ cells. Scale bar, 50 μm.
(C) CK^-p53^+ cells do not express CD11b. Scale bar, 25 μm.
(D) CK^-p53^+ cells do not express CD31. Scale bar, 25 μm.

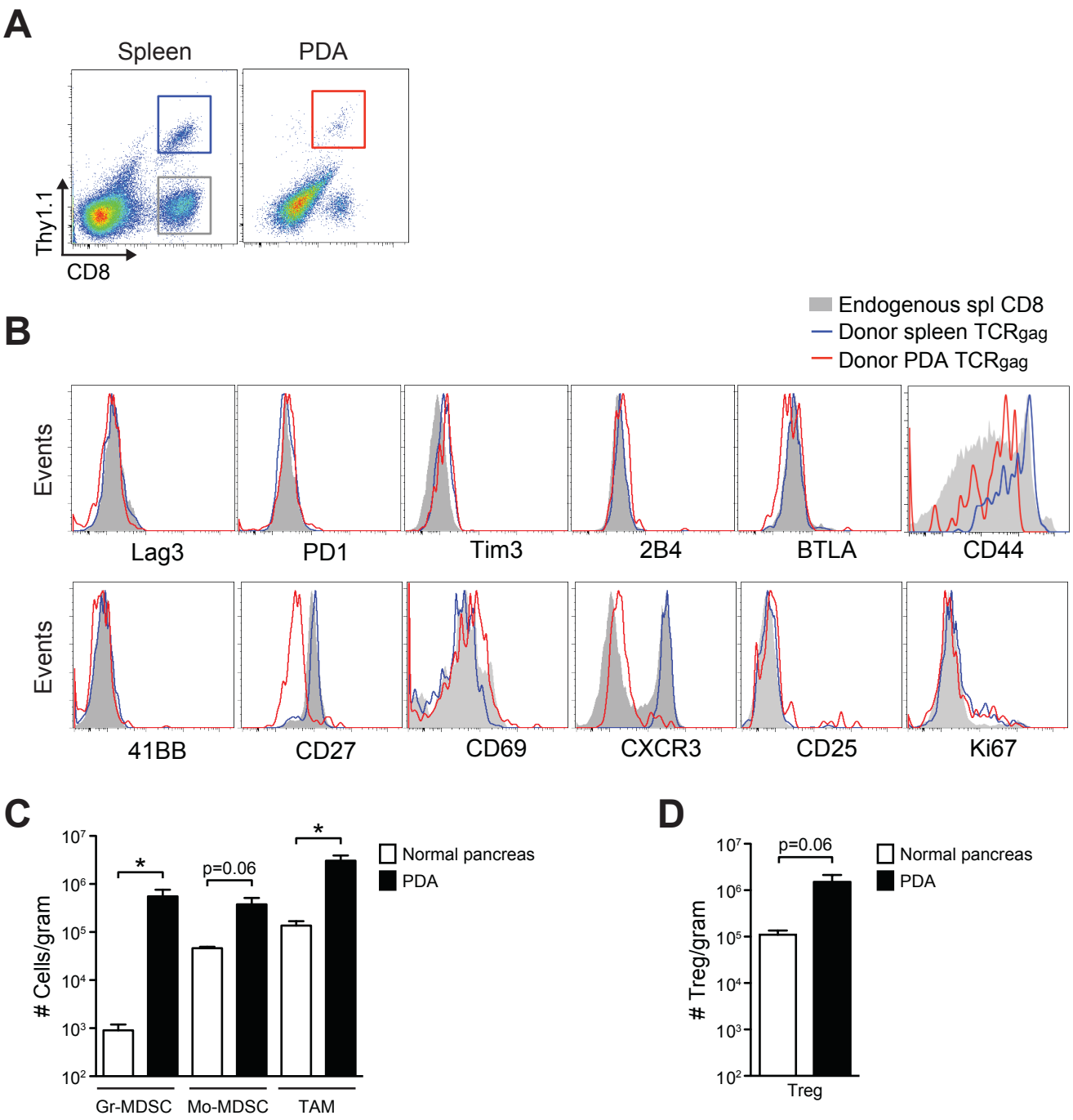

Figure S4, related to Figure 4.
(A) Gating of TCR_{gag} cells 8 days post transfer. Plots are gated on live $CD45^+$ cells.
(B) Phenotype of TCR_{gag} T cells 8 days post transfer.
(C) Number of granulocytic MDSC (Gr-MDSC, $CD45^+CD11b^+Gr1^{high}Ly6C^{int}$), monocytic MDSC (Mo-MDSC, $CD45^+CD11b^+Gr1^{int}Ly6C^{high}$) and tumor associated macrophages (TAM, $CD45^+CD11b^+Gr1^-Ly6C^{int}$) in normal pancreas and *KPC* PDA.
(D) Number of $CD45^+CD4^+Foxp3^+$ cells in normal pancreas and *KPC* PDA.
Data are shown as mean ± SEM and representative of n=3-7 mice each.

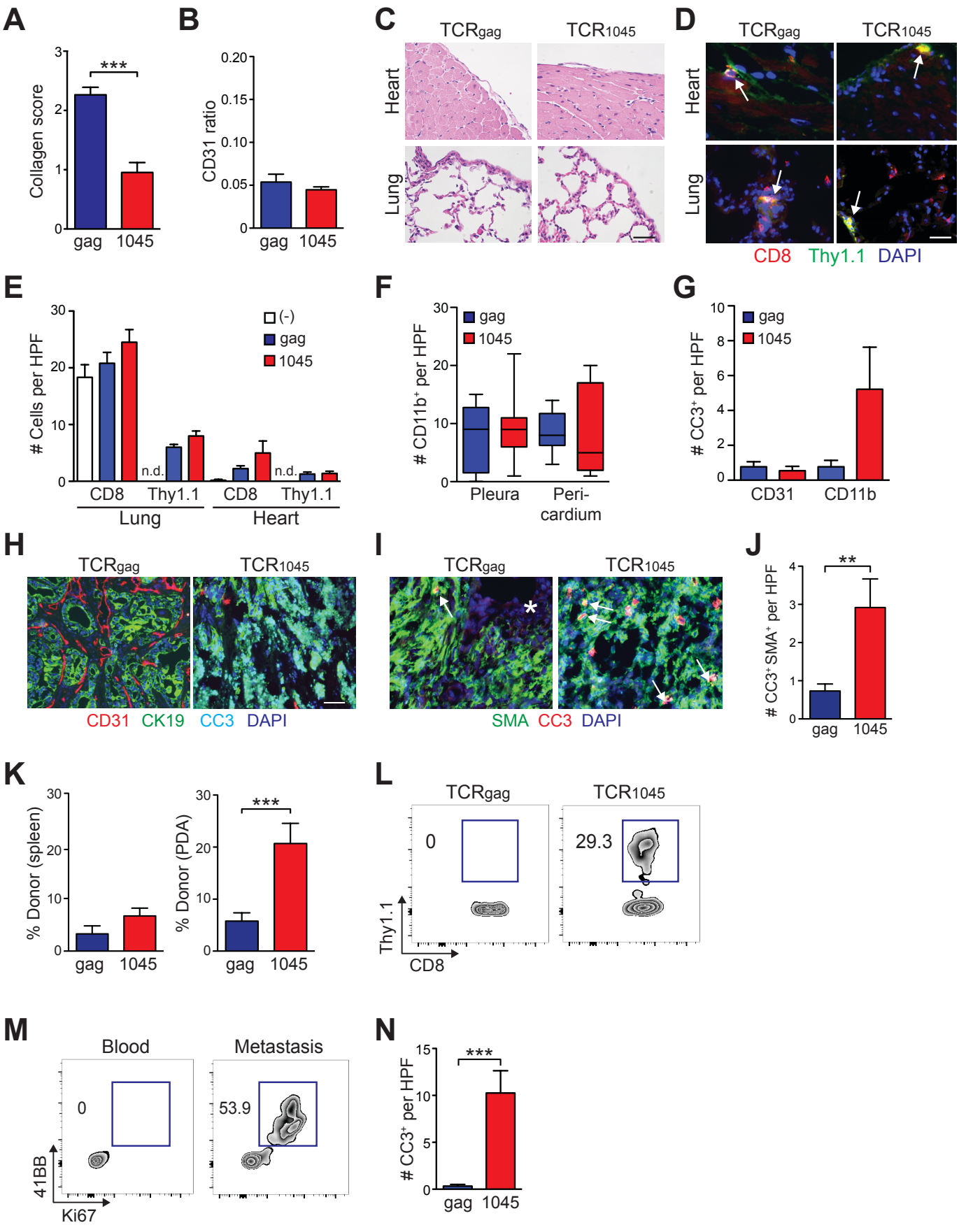
A
Collagen score
***
gag
1045
B
CD31 ratio
gag
1045
C
TCRgag
TCR1045
Heart
Lung
D
TCRgag
TCR1045
Heart
Lung
CD8 Thy1.1 DAPI
E
Cells per HPF
(-)
gag
1045
n.d.
n.d.
CD8
Thy1.1
CD8
Thy1.1
Lung
Heart
F
CD11b+ per HPF
gag
1045
Pleura
Peri-cardium
G
CC3+ per HPF
gag
1045
CD31
CD11b
H
TCRgag
TCR1045
CD31 CK19 CC3 DAPI
I
TCRgag
TCR1045
SMA CC3 DAPI
J
CC3+SMA+ per HPF
**
gag
1045
K
% Donor (spleen)
gag
1045
% Donor (PDA)
***
gag
1045
L
TCRgag
TCR1045
0
29.3
Thy1.1
CD8
M
Blood
Metastasis
0
53.9
41BB
Ki67
N
CC3+ per HPF
***
gag
1045

Figure S5, related to Figure 6.
(A) Quantification of collagen in PDA, related to Figure 6C.
(B) Quantification of CD31 in PDA, related to Figure 6C.
(C) Histology of lung and heart following multiple T cell infusions. Scale bar, 25 μm.
(D) Localization of donor ($CD8^+Thy1.1^+$) and endogenous ($CD8^+Thy1.1^-$) T cells in lung and heart. Arrows, $CD8^+Thy1.1^+$ donor T cells. Scale bar, 10 μm.
(E) Number of donor and endogenous CD8 T cells in lung and heart. n.d., not detected.
(F) Number of $CD11b^+$ cells in pleura and pericardium.
(G) Number of apoptotic endothelial ($CD31^+CC3^+$) and myeloid ($CD11b^+CC3^+$) cells.
(H) Absence of $CD31^+$ cells in regions of high tumor cell apoptosis in recipients of TCR_{1045} cells. Scale bar, 50 μm.
(I) Fibroblast apoptosis in PDA following TCR_{1045} cell therapy. Scale bar, 25 μm; *, tumor cells; arrows, αSMA^+CC3^+ cells.
(J) Number of αSMA^+CC3^+ cells, related to Figure S5I.
(K) Frequency of donor T cells at endpoint.
(L) Frequency of donor T cells in diaphragm metastases.
(M) Phenotype of TCR_{1045} T cells infiltrating metastases. Plots are gated on $CD8^+Thy1.1^+$ cells.
(N) Number of apoptotic tumor cells in metastases.
Data are shown as mean ± SEM and representative of n=3-13 mice each.

Table S1, related to Figure 6. Clinical spectrum of disease following treatment

ID	Survival from start of therapy (days)	Metastatic Disease					
		Liver	Lung	Diaphragm	Ascites	Cachexia	Other
A. TCR_{gag} (Control)							
1	18	*	*	*	*	*	
2	23	N	N	N	Y	N	
3	25	N	N	N	N	N	Neurological[§]
4	75	N	Y^M	Y^m	Y	Y	
5	24	*	*	*	*	*	
6	66	Y^m	N	nd	Y	Y	
7	70	N	N	N	N	Y	
8	86	Y^m	N	Y^M	Y	N	
9	76	Y^m	N	N	N	Y	
10	49	N	Y^m	N	Y	Y	
11	58	Y^M	N	N	N	Y	
12	35	N	N	N	N	N	
13	63	Y^m	N	nd	N	Y	
14	24	Y^m	Y^m	N	Y	Y	
15	35	N	N	N	N	Y	
16	64	Y^M	N	nd	N	Y	
B. TCR_{1045} (Mesothelin)							
1	101	N	N	N	N	Y	
2	112	*	*	*	*	*	
3	101	N	N	N	N	N	
4	93	Y^M	N	N	Y	N	
5	96	*	*	*	*	*	
6	46	N	N	N	Y	N	
7	21	N	N	N	N	N	Neurological[§]
8	80	N	N	N	N	Y	
9	99	N	N	Y^M	N	Y	
10	52	Y^m	N	N	N	Y	
11	155	N	Y^m	N	N	Y	
12	140	N	N	nd	N	Y	
13	84	N	N	N	N	N	Lymphoma[#]
14	74	N	N	Y^M	N	N	Lymphoma[#]
15	122	N	N	Y^M	N	Y	

[M], macrometastasis; [m], micrometastasis; *, tissue not evaluable secondary to necrosis; nd, not determined; [§], neurological signs included head tilt, ambulating in circles and/or hind limb ataxia likely secondary to CNS expression of *p48* (Sellick et al., 2004) and a loss of one p48 allele in *KPC* mice. [#], Lymphomas frequently occur in mice that are heterozygous or homozygous null for *Trp53* (Donehower et al., 1992; Jacks et al., 1994) and did not arise from engineered T cells.

Table S2, related to Figure 7. Human Mesothelin CD8 T cell epitopes

Epitope	HLA restriction	Human Sequence	BIMAS[#]	SYFPEITHI[#]	Reference
$MSLN_{153-161}$	HLA-A1	RGAPERQRL	0.025	3	(Lutz et al., 2011)
$MSLN_{158-166}$	HLA-A1	RQRLLPAAL	0.000	1	(Lutz et al., 2011)
$MSLN_{175-183}$	HLA-A1	LLSEADVRA	0.020	3	(Lutz et al., 2011)
$MSLN_{182-190}$[§]*	HLA-A1	RALGGLACD	0.02	3	(Lutz et al., 2011)
$MSLN_{217-225}$	HLA-A1	DQQEAARAA	0.002	1	(Lutz et al., 2011)
$MSLN_{224-232}$	HLA-A1	AALQGGGPP	0.001	3	(Lutz et al., 2011)
$MSLN_{309-317}$	HLA-A1	EIDESLIFY	125	25	(Thomas et al., 2004)
$MSLN_{20-28}$[§£]	HLA-A2	SLLFLLFSL	1054	30	(Thomas et al., 2004)
$MSLN_{80-88}$[§]	HLA-A2	RVRELAVAL	0.582	20	(Lutz et al., 2011)
$MSLN_{116-125}$[§]*	HLA-A2	ALPLLLLFL	270	28	(Hung et al., 2007a)
$MLSN_{159-167}$[§]	HLA-A2	QRLLPAALA	0.003	9	(Lutz et al., 2011)
$MSLN_{220-228}$[§]	HLA-A2	EAARAALQG	0.000	4	(Lutz et al., 2011)
$MSLN_{223-231}$[§]	HLA-A2	RAALQGGGP	0.000	7	(Lutz et al., 2011)
$MSLN_{530-538}$[§£]	HLA-A2	VLPLTVAEV	271	29	(Thomas et al., 2004)
$MSLN_{540-549}$	HLA-A2	KLLGHVEGL	312	30	(Hung et al., 2007a)
$MSLN_{83-91}$	HLA-A3	ELAVALAQK	9	27	(Thomas et al., 2004)
$MLSN_{225-233}$	HLA-A3	ALQGGGPPY	6	26	(Thomas et al., 2004)
$MSLN_{435-443}$	HLA-24	FYPGYLCSL	300	4	(Thomas et al., 2004)
$MSLN_{475-483}$	HLA-24	LYPKARLAF	150	9	(Thomas et al., 2004)

[#]HLA peptide binding predictions were performed using BIMAS (http://www.bimas.cit.nih.gov/molbio/hla_bind/) and SYFPEITHI (http://www.syfpeithi.com/).
[§]Attempted expansion of T cell clones specific to these epitopes
*Similar amino acid sequence between human and murine MSLN
[£]Successful isolation of numerous T clones specific to these epitopes

SUPPLEMENTAL EXPERIMENTAL PROCEDURES

TCR transduction of murine T cells

The ecotropic retroviral packaging cell line, Platinum (Plat)-E cells (Cell Biolabs, Inc.*)*, were plated ($2.2x10^6$ cells) in Plat-E media (DMEM, 10% FBS, 10 μg/ml blasticidin, 1 μg/ml puromycin, 100 U/ml penicillin/streptomycin) on 10 mm plates. After 24 h, Plat-E cells were transduced with retroviral vectors using Effectene (Qiagen). At 48 h, media was replaced with T cell media (DMEM, 10% FBS, 2 μM L-glutamine, 100 U/ml penicillin/streptomycin, 25 μM 2-β-mercaptoethanol) and virus-containing supernatant was collected on days 2 and 3 post-transfection. Splenic T cells isolated from P14 $Thy1.1^+$ female mice were stimulated with αCD3 (145-2C11) and αCD28 (37.51) (BD Biosciences) and IL-2 (50 IU/ml, NIH), and transduced with retroviral supernatant by spinfection (90 min at 1000 *g*) 24 and 48 hr following T cell activation in polybrene. Transduced T cells were re-stimulated with irradiated $Thy1.2^+$ splenocytes pulsed with $MSLN_{406-414}$ peptide (GQKMNAQAI, 1 μg/ml) and recombinant human IL-2 (r-IL2, 50 IU/ml) seven days following T cell activation with anti-CD3/CD28. On day 5 after antigen re-stimulation, >90% T cells expressed the introduced TCR and a total of $1x10^7$ $tetramer^+$ cells were infused.

Adoptive immunotherapy

KPC mice underwent serial high-resolution ultrasound imaging (Vevo 2100) at 8 weeks of age to monitor autochthonous tumor development. Mice were enrolled based on defined pancreatic mass 3-6 mm; disease was frequently palpable and diffusely multifocal. The average tumor diameter at enrollment was not significantly different between the two treatment arms: TCR_{gag} cohort, 3.8 ± 0.6 mm; TCR_{1045} cohort, 3.5 ± 0.5 mm. The mean age of mice at enrollment was also similar: TCR_{gag} cohort, 105 ± 5 days; TCR_{1045} cohort, 98 ± 6 days. Mice were randomized by one investigator and treated by a second. Animals received cyclophosphamide once at enrollment (180 mg/kg) followed 6 hr later by intravenous infusion of $1x10^7$ twice-stimulated engineered T cells followed by $1x10^7$ peptide-pulsed irradiated splenocytes. Recipient mice received IL-2 ($2x10^4$ IU, i.p.) every other day for 8 days (in timepoint studies) or for 5 days (in survival studies) to promote donor T cell survival and expansion. For serial T cell infusions, mice received the same treatment protocol, excluding the

cyclophosphamide after the first dose, every 2 weeks. Power analyses guided enrollment numbers to power the study for a large effect (>50% increase in median OS).

Ultrasound imaging

By virtue of the targeting strategy, cancers in the *KPC* model arise stochastically from precursor lesions and progress spontaneously to create multifocal disease. High-resolution ultrasound imaging was used to identify a dominant mass that met enrollment criteria and served also as the potential target lesion for objective response (OR) measurements. OR is reported for the subset of target lesions that could be followed with confidence on subsequent examinations. We note that lesions arise amidst the backdrop of a continuously evolving multifocal and multinodular disease process. Anatomic landmarks used to reliably follow an identified target lesion over time were as follows: for the pancreatic head, the right kidney, liver portal vein, duodenum and inferior vena cava; for the pancreatic body, the portal vein, aorta, stomach and splenic vein; for the pancreatic tail, the spleen, stomach and left kidney. Ultrasound measurements were performed independently and in a blinded fashion by two investigators (C.C. and I.M.S.; C.C. is an attending radiologist and abdominal imaging specialist who has over 6 years experience imaging *KPC* mice). Tumor volume ($4/3\pi r^3$) was estimated using radius as determined by the average of two cross-sectional diameters.

Primary cells and cell lines

Primary *KC* (preinvasive) and *KPC* invasive PDA cells derived from 129Sv/Bl/6 mixed background animals (Hingorani et al., 2003; Hingorani et al., 2005) were used for immunoblots in Figure 1E. The murine immature thymoma cell lines E10 (Mombaerts et al., 1995) and 58 $TCR\alpha\beta^{-/-}$ (Letourneur and Malissen, 1989) have been described. The murine pancreas cancer cell line Panc02 and immortalized human Jurkat-76, 293T and T2 cell lines were purchased from American Type Culture Collection (ATCC, Rockville, MD). The human Panc-1 pancreas cancer cell line was a gift from Translational Genomics (Phoenix, AZ). Immortalized Human Ductal Pancreatic Epithelial (HPDE) cells were a gift from Dr. Tsao (University Health Network, Ontario, Canada) (Furukawa et al., 1996; Ouyang et al., 2000).

Assessment of primary and metastatic disease burden

Study animals underwent full necropsies including gross examination of all organs for macroscopic disease. Harvested tissues were fixed in 10% neutral buffered formalin, embedded in paraffin, sectioned (4 μm) and used for various immunohistochemical and histochemical assays.

Histology and immunohistochemistry (IHC)

Tissues were fixed in 10% formalin and embedded in paraffin. Sections (4 μm) were stained with hematoxylin and eosin (H&E) or Masson's trichrome. Primary antibodies used include MSLN 1:100 (human: LSB2618, LSBio; mouse: 308, IBL), WT1 1:100 (human, 6F-H2, DAKO; mouse, polyclonal, Thermo Scientific), ANXA2 1:500 (3H1B11, proteintech), MUC1 1:100 (CT2, abcam) and CD31 1:200 (BD Biosciences 390). Slides were scanned in brightfield with 20X objective using a Nanozoomer Digital Pathology slide scanner (Hamamatsu; Bridgewater, New Jersey). The digital images were imported into Visiopharm software (Hoersholm, Denmark) and analyzed after identifying regions of interest (ROI, i.e. tumor tissue, individual metastases) and excluding normal tissue. The software was trained to detect immunoreactivity using a project-specific configuration based on a threshold of pixel values. The ROI were sampled at 100 percent. The mean vessel diameter (MVD) of $CD31^+$ vessels was measured in 3-5 non-overlapping 20X fields using NIS-Element imaging software and 100-130 vessels were assessed per group (n=3-5 mice). For quantification of collagen, tumor sections from 3-6 animals per cohort were reacted with Masson's trichrome and intensity of the blue staining assessed in a blinded manner across 3-5 20X fields as follows: 0, no staining detected; 1, light staining; 2, moderate; 3, high staining intensity.

Immunofluorescence

Tissues were embedded and frozen in OCT and stored at -80°C. Sections (7 μM) were fixed in cold (-20°C) acetone for 15 min. Slides were rehydrated with PBS+2% BSA, blocked with 2% goat serum and incubated for 1 hr at room temperature with the primary antibody diluted in PBS+2.5% BSA. Primary antibodies used include MSLN (MBL B35, 1:100), pan-CK-FITC (Sigma-Aldrich F3418,

1:200), CD8α (BD Biosciences 53-6.7, 1:25), p53 (Thermo Scientific, DO-7 1:200), CC3 (Cell Signaling D175, 1:200), αSMA (Dako 1A4, 1:100), Thy1.1 (BD Biosciences OX-7, 1:25), CD11b (eBioscience M1/70, 1:25), E-Cadherin (R&D Systems, 1:100) and CD31 (eBioscience 390, 1:50). Slides were incubated with species-specific secondary Alexa-conjugated antibodies (Invitrogen, 1:1000) and mounted with Prolong Gold anti-fade plus DAPI (Life Technologies). Quantification of apoptosis was performed blinded by counting dual labeled cells in 3-5 high power fields (HPF; 40X) from 3-8 mice per group.

Isolation of mononuclear cells from tissues

Spleens were disrupted by mechanical force through a 70 μm filter and red blood cells lysed using ACK lysis buffer. Pancreatic tumors were excised and peri-pancreatic lymph nodes and normal adjacent tissue removed using a dissecting scope. Tumors were minced, incubated for 30 min in 1 mg/ml collagenase (Sigma) at 37°C, washed in DMEM/F12 10% FBS, and strained through a 100 μm filter.

Generation of primary pancreatic tumor epithelial cells

Cells and tissue fragments retained on the 100 μm filter during the isolation of mononuclear cells from pancreatic tumors (described above) were collected and plated on collagen at 37°C in DMEM/F12, 10% FBS and 2.5 g D-glucose and Pen/Strep (Basic Media). Primary B6 *KPC* tumor epithelial cells were passaged less than 5 times prior to analyses to ensure fidelity to the autochthonous tumor. All cell lines are routinely tested for Mycoplasma contamination using LookOut Mycoplasma PCR Detection Kit (Sigma).

Antibodies for flow cytometry

Fluorophore-conjugated antibodies were purchased from BD Biosciences: CD45 (30-F11), CD8α (53-6.7), Thy1.1 (OX-7), Thy1.2 (53-2.1), Ki67 (B56), Tim3 (RMT3-23), CD27 (LG.7F9), CD69 (H1.2F3), CD3 (145-2C11), CD28 (37.51) and CD44 (IM7). Antibodies to 41BB (17B5), PD1 (J43), CD25 (PC61), 2B4 (eBio244F4), BTLA (6F7), Lag3 (C9B7W), IFNγ (XMG1.2), TNFα (MP6-XT22), H-2D^{b} (28-

14-8) and CD31 (390) were purchased from eBioscience. The $MSLN_{406-414}$/H-$2D^b$, $MSLN_{20-28}$/HLA-A2 and $MSLN_{530-538}$/HLA-A2 tetramers conjugated to APC were produced in the Fred Hutch Immune Monitoring Core. MSLN peptides were purchased from Pi proteomics.

Quantitative PCR

Total RNA was extracted from primary tumor epithelial cells (n=7 independent tumors) or tissues using the RNeasy Miniprep Kit (Qiagen) according to the manufacturer's suggestions. High capacity reverse transcriptase (Applied Biosystems) converted RNA to cDNA. Quantitative PCR was performed using SYBR Green (Applied Biosystems) and samples were run in triplicate on a C1000 thermal cycler (Biorad). Primers for amplification of murine genes: MSLN sense, 5'-ACAACGCAGCTGATGTCCCCG-3'; MSLN antisense, 5'-GGAGGCCCCACCCAGGAATGT-3'; *cycA* sense, 5'-GAGCTGTTTGCAGACAAAGTTC-3', *cycA* antisense, 5'-CCCTGGCACATGAATCCTGG-3'; CK19 sense: 5'-GTCCTACAGATTGACAATG-3'; CK19 antisense: 5'-CACGCTCTGGATCTGTGACAG-3'. Data was normalized to the housekeeping gene *cycA*. Primers used for human genes have been described (Bharadwaj et al., 2011): hMSLN sense: 5'-CTCAACCCAGATGCGTTCTCG-3'; hMSLN antisense: 5'-AGGTCCACATTGGCCTTCGT-3'; hGAPDH sense: 5**'**-TGCACCACCAACTGCTTAGC-3**'**; hGAPDH antisense: 5**'**-GGCATGGACTGTGGTCATGAG-3**'**.

CD8-independent murine tetramer binding

The $CD8^-$ 58 TCR$\alpha\beta^{-/-}$ thymoma cell line (Letourneur and Malissen, 1989) was transduced with CD8α and β and either TCR_{7431} or TCR_{1045}. Transduced cells were stained for CD8α, Vβ9 and $MSLN_{406-414}$/H-$2D^b$ tetramer for 30 min on ice. Expression of the introduced TCR was determined by comparing tetramer staining of $CD8^+$ and $CD8^-$ V$\beta9^+$ populations.

Tetramer dissociation assay

P14 T cells transduced to express either TCR_{7431} or TCR_{1045} were stained for CD8, Vβ9 and $MSLN_{406-414}$/H-$2D^b$ tetramer (0.5 μg/ml). At time 0, saturating concentrations (50 μg/ml) of unlabeled

$MSLN_{406-414}$/H-$2D^b$ tetramer were added and the cells sequentially acquired by flow cytometry at room temperature. The MFI of tetramer staining was normalized to time 0.

Cloning murine Mesothelin-reactive T cells

B6 and $MSLN^{-/-}$ mice (n=5 each) were injected with $5x10^8$ pfu of a recombinant attenuated adenovirus vaccine (i.m.) engineered to express recombinant murine Mesothelin (Ad-MSLN). At day 30, mice were boosted with $5x10^8$ pfu of Ad-MSLN. Seven days later, mice were euthanized and spleens harvested for mononuclear cells. Cells were cultured with the following 9mer peptides selected based on published studies (Hung et al., 2007b; Leao et al., 2008) at 1 µg/ml: $MSLN_{146-154}$, $MSLN_{353-341}$, $MSLN_{350-358}$, $MSLN_{406-414}$, $MSLN_{484-492}$, $MSLN_{544-552}$, $MSLN_{583-591}$, and $MSLN_{612-619}$. IL-2 (25 IU/ml) was added on the day of antigen stimulation only. $Thy1.2^+$ T cells ($1x10^6$) were re-stimulated every 7 days with irradiated peptide-pulsed $Thy1.1^+$ splenocytes ($1x10^7$) and IL-2 (25 IU/ml) until a pure population of MSLN-reactive T cells was obtained as measured by tetramer and intracellular cytokine staining (ICS). After 4 sequential stimulations, $MSLN_{406-414}$-specific T cell lines derived from WT and $MSLN^{-/-}$ mice were cloned by limiting dilution. Tetramer staining intensity and functional avidity (ICS) of T cell clones (10-15 per strain) were compared. The highest affinity clone isolated from the $MSLN^{-/-}$ mice (1045) and from WT mice (7431) were selected for TCR isolation.

FACs analyses for p53

Tumor cells were first immunolabeled with the surface antigens MSLN, MHC class I, and CD45 in PBS+2.5% FBS (FACs buffer). Cells were washed in FACs buffer and fixed and permeabilized using eBioscience Fixation/Permeabilization buffers as specified. Permeabilized cells were resuspended in rabbit anti-p53 mAb (Thermo Scientific, DO-7 1:200), diluted in eBioscience 1X Permeabilization buffer and incubated for 30 min on ice. Labeled cells were then washed x2 in eBioscience Permeabilization buffer and resuspended in anti-rabbit 647 (1:1000, Invitrogen) and analyzed on a FACSCanto II.

Intracellular cytokine production

Mononuclear cells ($1x10^6$) isolated from the spleen or primary tumors were incubated for 5 hr in Golgiplug (BD Biosciences) ± $MSLN_{406-414}$ peptide. Cells were then reacted in the dark with antibodies to CD8 (1:200) and Thy1.1 (1:200) diluted in FACs buffer for 30 min on ice. Cells were washed x2 with FACs buffer and fixed for 20 min on ice with BD Biosciences Fix/Perm. Cells were washed with 1X BD Biosciences Perm/Wash and incubated with antibodies to IFNγ (1:100) and TNFα (1:100) for 30 min on ice. All FACs data were acquired using a FACSCanto II.

Immunoblots

Immunoblots for MSLN (Santa Cruz clone K1, 1:1000) and actin (Santa Cruz goat polyclonal, 1:1000) were performed on normal, preinvasive (*KC*) and invasive (*KPC*) lysates as described (Hingorani et al., 2005).

Cloning and expansion of human MSLN-reactive T cells

After obtaining informed consent, peripheral blood mononuclear cells (PBMC) were harvested from 5 normal HLA-$A2^+$ donors. $CD8^+$ T cells purified using Miltenyi magnetic beads were stimulated with autologous, irradiated monocyte-derived dendritic cells loaded with MSLN peptides (Table S2). A rapid expansion protocol was used to expand T cell clones as we have previously described (Ho et al., 2006).

Cloning human MSLN-reactive TCRs

The MSLN-specific TCR expression cassette consists of codon-optimized TCRα and TCRβ genes derived from HLA-A2-restricted CD8 T cell clones specific to $MSLN_{20-28}$ or $MSLN_{530-538}$. The TCRα and TCRβ genes are linked by a 2A element from porcine teschovirus (P2A) to ensure coordinated expression under the control of the murine stem cell virus (MSCV) U3 promoter. The TCR expression construct MesoTCRα-P2A-TCRβ was ligated into the third-generation, self-inactivating lentiviral vector pRRLSIN.cPPT.MSCV/GFP.WPRE (gift from Richard Morgan) between the AscI and SalI restriction sites, replacing GFP.

TCR transductions of human T cells

To generate lentiviruses, 293 T cells ($3x10^6$ cells/plate) were transduced with pRRLSIN-MSLNTCRα-P2A-TCRβ constructs and the packaging vectors pMDLg/pRRE, pMD2-G and pRSV-REV using Effectene (Qiagen). Culture media was changed on day 1 post-transfection and virus-containing supernatant collected on days 2 and 3, and aliquots frozen for future use. Human $CD8^+$ T cells were purified from PBMCs by magnetic bead separation *(*Miltenyi) and stimulated in the presence of 50 IU/ml IL2 using Human T cell Expander CD3/CD28 Dynabeads (Life Technologies). 4-6 hr and 24 hr following stimulation, $2x10^6$ cells were spinfected with 2 ml of retroviral supernatant at 1000 *g* for 90 min at 32°C. Jurkat T cells lacking endogenous TCRα and TCRβ chains were transduced in a similar manner without prior stimulation.

Biodistribution of T cells *in vivo*

Mice were treated with Nair to remove hair and injected with 150 mg/kg D-Luciferin (Life technologies). Images were acquired at 30 sec, 1 min, 5 min and 12 min using the IVIS Spectrum (Perkin Elmer) and the bioluminescent signal quantified using Living Image 4.3.1 (Perkin Elmer). To visualize engineered T cells, P14 T cells were co-transduced with the TCR vector and a vector encoding click beetle red (CBR, provided by Dr. Matthias Stephan (Fred Hutch)). Only a fraction of donor T cells concurrently expressed CBR (~5-10%) but this was sufficient for *in vivo* imaging.

Intracellular cleaved-caspase 3 staining

Primary tumor epithelial cells ($1x10^5$) derived from B6 *KPC* PDA were labeled with 5-6-carboxyfluorescein diacetate succinimidyl ester (CFSE, 10 μM, eBioscience) and incubated overnight in flat bottom plates. The next day, labeled adherent tumor cells were incubated with engineered T cells ($1x10^6$) for 5 hr. Cells were trypsinized (0.25% Trypsin, 5 min at 37°C), stained with CD45-Percp (1:200), fixed and permeabilized (BD Biosciences Fix/Perm) and stained for intracellular CC3 (1:100). CC3 expression was determined by gating on $CFSE^+CD45^-$ tumor cells.

SUPPLEMENTAL REFERENCES

Bharadwaj, U., Marin-Muller, C., Li, M., Chen, C., and Yao, Q. (2011). Mesothelin confers pancreatic cancer cell resistance to TNF-alpha-induced apoptosis through Akt/PI3K/NF-kappaB activation and IL-6/Mcl-1 overexpression. Mol Cancer *10*, 106.

Donehower, L. A., Harvey, M., Slagle, B. L., McArthur, M. J., Montgomery, C. A., Jr., Butel, J. S., and Bradley, A. (1992). Mice deficient for p53 are developmentally normal but susceptible to spontaneous tumours. Nature *356*, 215-221.

Furukawa, T., Duguid, W. P., Rosenberg, L., Viallet, J., Galloway, D. A., and Tsao, M. S. (1996). Long-term culture and immortalization of epithelial cells from normal adult human pancreatic ducts transfected by the E6E7 gene of human papilloma virus 16. Am J Pathol *148*, 1763-1770.

Ho, W. Y., Nguyen, H. N., Wolfl, M., Kuball, J., and Greenberg, P. D. (2006). In vitro methods for generating CD8+ T-cell clones for immunotherapy from the naive repertoire. J Immunol Methods *310*, 40-52.

Hung, C. F., Calizo, R., Tsai, Y. C., He, L., and Wu, T. C. (2007). A DNA vaccine encoding a single-chain trimer of HLA-A2 linked to human mesothelin peptide generates anti-tumor effects against human mesothelin-expressing tumors. Vaccine *25*, 127-135.

Jacks, T., Remington, L., Williams, B. O., Schmitt, E. M., Halachmi, S., Bronson, R. T., and Weinberg, R. A. (1994). Tumor spectrum analysis in p53-mutant mice. Curr Biol *4*, 1-7.

Leao, I. C., Ganesan, P., Armstrong, T. D., and Jaffee, E. M. (2008). Effective depletion of regulatory T cells allows the recruitment of mesothelin-specific CD8 T cells to the antitumor immune response against a mesothelin-expressing mouse pancreatic adenocarcinoma. Clin Transl Sci *1*, 228-239.

Lutz, E., Yeo, C. J., Lillemoe, K. D., Biedrzycki, B., Kobrin, B., Herman, J., Sugar, E., Piantadosi, S., Cameron, J. L., Solt, S.*, et al.* (2011). A lethally irradiated allogeneic granulocyte-macrophage colony stimulating factor-secreting tumor vaccine for pancreatic adenocarcinoma. A Phase II trial of safety, efficacy, and immune activation. Ann Surg *253*, 328-335.

Mombaerts, P., Terhorst, C., Jacks, T., Tonegawa, S., and Sancho, J. (1995). Characterization of immature thymocyte lines derived from T-cell receptor or recombination activating gene 1 and p53 double mutant mice. Proc Natl Acad Sci U S A *92*, 7420-7424.

Ouyang, H., Mou, L., Luk, C., Liu, N., Karaskova, J., Squire, J., and Tsao, M. S. (2000). Immortal human pancreatic duct epithelial cell lines with near normal genotype and phenotype. Am J Pathol *157*, 1623-1631.

Sellick, G. S., Barker, K. T., Stolte-Dijkstra, I., Fleischmann, C., Coleman, R. J., Garrett, C., Gloyn, A. L., Edghill, E. L., Hattersley, A. T., Wellauer, P. K.*, et al.* (2004). Mutations in PTF1A cause pancreatic and cerebellar agenesis. Nat Genet *36*, 1301-1305.